Mon. Not. R. astr. Soc. (1992) **258**, 483–490

Probing photoionization models in two well-studied extended emission-line regions: Centaurus A and 3C 227

Sueli M. Viegas[1,2] and M. Almudena Prieto[3]★

[1] *European Southern Observatory, Karl Schwarzschild Straße 2, D-8046, Garching bei München, Germany*
[2] *Instituto Astronômico e Geofísico, USP, Av. Miguel Stefano 4200, 04301-São Paulo, SP, Brazil*
[3] *Space Telescope European Coordinating Facility, ESO, Karl Schwarzschild Straße 2, D-8046, Garching bei München, Germany*

Accepted 1992 March 23. Received 1992 March 16; in original form 1991 November 18

SUMMARY

The observed emission-line ratios of the extended emission-line regions of Cen A and 3C 227 are compared with the theoretical results from photoionization models, assuming a power-law spectrum for the nuclear ionizing radiation. We show that a variation of the optical depth of the emitting gas can mimic a variation of the ionization parameter. Most of the observational data are explained if each subregion in the extended emission-line gas is characterized by a different value of the optical depth and shows a small density contrast between a 'cloud' and a more dilute gas. However, the observed [O III] line ratio cannot be reproduced by photoionization, and an additional heating mechanism is required. Solar abundances give the best fit to the observations. However, for most subregions the [N/O] ratio is between solar and half solar.

Key words: line: formation – radiative transfer – galaxies: abundances – galaxies: active – galaxies: individual: Cen A – galaxies: individual: 3C 227.

1 INTRODUCTION

In recent years, regions of extended ionized gas have been detected in different types of active galaxies. The extra-nuclear line emission is usually associated with radio emission, and extends from a few kpc to a few hundred kpc (Baum & Heckman 1989; Whittle 1989). Imaging of these regions shows an asymmetrical morphology, sometimes with a biconical or cylindrical structure suggesting that the nuclear radiation source is anisotropic and providing support for the so-called unified models for active galactic nuclei (Fosbury 1989; Pogge 1989).

The analysis of the emission-line spectra of the extra-nuclear ionized gas is a tool to understanding the nature of these regions, as well as of the nuclear radiation source. Photoionization of the gas by either a power-law or a black-body radiation source can reproduce the main features of the observed emission-line spectra of the extended regions (Robinson *et al.* 1987). However, in order to explain some of the observed line ratios and the spread of the data on the diagnostic diagrams, more sophisticated models have to be considered.

Detailed analysis of the optical filaments of Centaurus A, based on long-slit spectroscopy and photoionization models, led to the conclusion that the spatial variations of the line intensity ratios are due to a local distribution of densities (Morganti *et al.* 1991). However, as we show here, the main point of the models presented by Morganti *et al.* is to allow for a local mixing of optically thick (radiation-bounded) and optically thin (matter-bounded) gas, rather than for a local distribution of densities.

The total opacity of the emission-line cloud to the ionizing continuum has different effects on different lines (Viegas-Aldrovandi 1988), and may enhance the problem of the deficit of ionizing photons which are required to explain the observed luminosities of the extended emission-line regions (Baum & Heckman 1989), setting tighter constraints on the anisotropy of the central source. The presence of optically thin filaments in the extended emission-line region (EELR) may affect the unified models for active galactic nuclei (AGN). In addition, when comparing theoretical and observational data, a variation of the optical depth of the gas can mimic a variation of the ionization parameter, producing misleading conclusions. Therefore, our aim is to study the effect of the optical depth, which seems to be very important in the analysis of the EELR. In order to test models of the emitting gas photoionized by the nuclear source, results from

★ Affiliated to the Astrophysics Division, Space Science Department, European Space Agency.

photoionization models, considering different ionization parameters and optical depths, are compared with observational data from the EELRs of two well-observed low-redshift radio galaxies.

2 THE EELRs OF CENTAURUS A AND 3C 227

Although the presence of EELRs seems to be a common phenomenon in active objects, in our analysis we compare photoionization models with observational data from two EELRs that have been observed in detail and for which rich emission-line spectra are available at different spatial positions (Morganti *et al.* 1991; Prieto *et al.*, in preparation).

Narrow-band imaging of Cen A (Morganti *et al.* 1991) shows bright blobs and filamentary structures in the north-western part of the galaxy, with position angles between 35° and 60°, in agreement with observed radio and X-ray structures (Feigelson *et al.* 1981; Burns *et al.* 1983). The main optical structures (inner and outer filaments) are situated at about 7.6 and 14.6 arcmin from the nucleus, showing a projected length of several kpc. The filaments show a complex velocity structure, with velocities between 120 and 300 km s^{-1}. Radio observations reveal a counter-jet, but no optical features are seen in the south-eastern part of Cen A. If the biconical structure is present, it must be hidden by the dust lane.

On the other hand, [O III] and Hα + [N II] imaging of 3C 227 shows a quite irregular EELR consisting of highly excited blobs and filaments (Prieto, di Seregho Alighieri & Fosbury 1989; Prieto *et al.*, in preparation). The ionized gas as a whole appears confined within the radio structure and rotating in the gravitational potential of the host galaxy, reaching velocities of up to 300 km s^{-1}. A biconical structure is suggested by the observed velocity field and the apparent morphology of the ionized gas.

The emission-line spectra of both EELRs are similar, with no continuum detected. Both show subregions with high He II λ4686 and [O I] λ6300 line intensities. The main difference comes from the fact that the Hα/Hβ ratio in Cen A's subregions suggests the presence of reddening, with c in the range 0.2 to 0.6, whereas observations of 3C 227 seem to be reddening-free. When necessary, we correct the line intensities for reddening using the observed Hα/Hβ ratio and assuming case B recombination. We recall that most of the emission-line ratios plotted in our diagrams are practically independent of reddening. Thus the observational data of Cen A and 3C 227 are distributed over a similar area. However, a clear segregation appears when the [O II] λ3727/[O III] λ5007 ratio is considered, which could be due to either a reddening overestimation in Cen A or abundance effects. We will discuss both possibilities in Section 4.

3 OPTICAL DEPTH EFFECTS

One of the problems faced by photoionization models of EELRs is the observed values of the He II λ4686/Hβ line ratio, which can be as high as 0.6. In standard photoionization models (radiation-bounded), this line ratio is mainly dependent on the spectral shape of the ionizing radiation. For a power-law spectrum, with power index $\alpha = 1.5$ (generally assumed for the nuclear radiation source), the He II/Hβ line ratio is of the order of 0.2, far below some observed values. A blackbody spectrum with temperature equal to 10^5 K does not provide larger values either. A flatter power law or hotter blackbody spectrum would increase this line ratio, but with two problems. First, they would provide a poor fit to the other emission lines, and secondly and more importantly, neither of them is able to reproduce the observed He II/Hβ trend (see Fig. 2). On the other hand, a shock effect could account for the large He II/Hβ values observed. However, shock models predict large He II ratios coupled with large [O III] ratios (Viegas & de Gouveia Dal Pino 1992), which differs from the observed trend.

If the gas is not optically thick to all the ionizing continuum (i.e., is matter-bounded), the H^+-emitting volume is smaller, but the He^{++} volume is not, leading to a higher He II/Hβ line ratio. This kind of model seems, therefore, promising for the EELR. However, because the volume of the low-ionization zone decreases with decreasing optical depth of the cloud, the intensities of low-ionization lines could be severely affected, while those of the high-ionization lines remain the same. This could compromise the model and must be analysed in more detail.

3.1 Photoionization models

In order to analyse quantitatively the effect on the observed lines of reducing the opacity to the ionizing continuum, we use the code AANGABA (recently updated by Gruenwald & Viegas 1992) to compute an extensive grid of photoionization models with different values of the opacity τ_0 (the optical depth at the Lyman limit) of the line-emitting cloud.

The input parameters are: (i) a power-law spectrum for the nuclear ionizing radiation, with a power index equal to 1.5 in the ultraviolet range and 0.70 in the X-ray range (Gruenwald & Viegas-Aldrovandi 1987), and characterized by a photoionization parameter in the range $6\times10^{-4} \leq U \leq 10^{-2}$; (ii) a total hydrogen density between 1 and 1000 cm^{-3}; (iii) different metallicities – solar (Grevesse & Anders 1989), cosmic (Allen 1973) and H II region (Shaver *et al.* 1983).

The upper limit on U is mainly due to the upper limit of the [O III] λ5007/Hβ line ratio observed in the EELR ($\leq$13). Although also affected by optical depth, this line ratio is a good indicator of the degree of excitation of the emitting gas, being proportional to U.

The [S II] line ratio observed in the EELR of Cen A indicates that the density is of the order of a few $\times 10^2$ cm^{-3}.

Previous photoionization models for the EELR point towards solar abundances (Robinson *et al.* 1987). Results considering chemical composition other than solar are discussed in Section 4.

For each set of input parameters, we calculate the emission-line intensities for τ_0 values ranging from optically thin ($\tau_0 < 1$) to optically thick ($\tau_0 \simeq 10^4$) cases. The thick case is generally considered to be achieved when the fraction of ionized hydrogen reaches 1 per cent (Binette 1985). We assume a plane-parallel geometry.

Let us notice that we shall be referring our results to the position in the cloud where the optical depth at the Lyman limit is equal to a given value of τ_0. The corresponding value of the neutral hydrogen column density can easily be obtained by $N(\mathrm{H\,I}) = \tau_0/a_0$ (a_0 being the hydrogen photoion-

ization cross-section at the threshold and equal to 6.3×10^{-18} cm^2).

3.2 Diagnostic diagrams

Because the [O II] λ3727/[O III] λ5007 line ratio is more affected by reddening correction and by optical depth effects than [O III] λ5007/Hβ, we have chosen this line ratio as an indicator of the degree of excitation of the emitting gas. The first four diagrams (Figs 1–4) show [O II] λ3727/[O III] λ5007, He II λ4686/Hβ, [N II] λ6584/Hα, and [O I] λ6300/Hα as a function of [O III] λ5007/Hβ (Figs 1 to 4).

The different symbols correspond to the observational data. All Cen A data are plotted as small filled triangles. On the other hand, data referring to 3C 227 are represented by different symbols according to several subregions in the gas. Basically, + symbols identify regions located further than 50 kpc from the nucleus, the other symbols identifying regions closer than 50 kpc characterized by different excitation levels (see caption of Fig. 1). The theoretical results correspond to solar abundances and are presented by lines: the dot–dashed line corresponds to optically thick models, the ticks (small squares) correspond to log $U = -3.2$, -3.0, -2.7, -2.5 and -2.0 dotted lines correspond to different values of τ_0, for a given value of U.

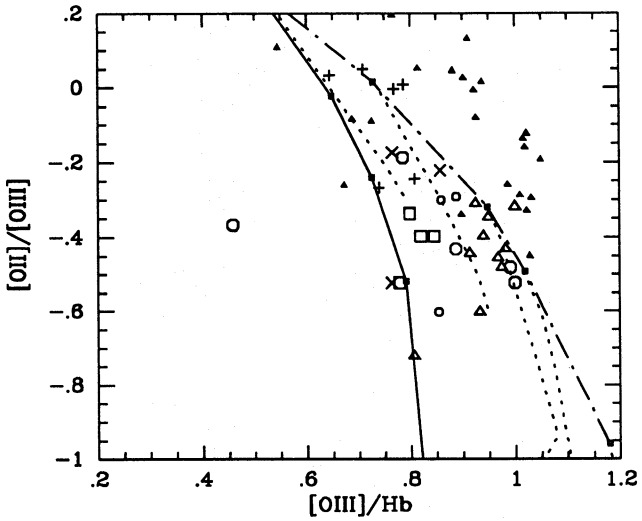

Figure 1. The [O II] λ3727/[O III] λ5007 versus [O III] λ5007/Hβ line ratios. The Cen A subregions (Morganti *et al.* 1991) are represented by the small filled triangles. The 3C 227 subregions are represented by different symbols according to their projected distance from the nucleus: + identify regions located more than 50 kpc, and other symbols (○, ○, △, □, ×) correspond to subregions less than 50 kpc from the nucleus. Each of them identifies a different spatially resolved subregion in the extended gas of 3C 227. The dot–dashed line corresponds to optically thick models, with hydrogen density $n_H = 10^2$ cm^{-3}, the ticks (small squares) correspond to ionization parameter equal to $10^{-3.2}$, $10^{-3.0}$, $10^{-2.7}$, $10^{-2.5}$, 10^{-2}. For the sake of clarity, the model with $U = 10^{-2}$ is not included in Fig. 1, but it is shown in the rest of the figures. For a given U, models varying the optical depth at the Lyman limit, from optically thin to opticaly thick cases, are shown as dotted lines. The solid line results from the combination of an optically thick filament, with $U = 10^{-3.2}$, and an optically thin model, with $U = 10^{-2}$; the ticks correspond to results considering the contribution of the filament to the emission-line spectrum to be equal to 70, 50 and 30 per cent respectively.

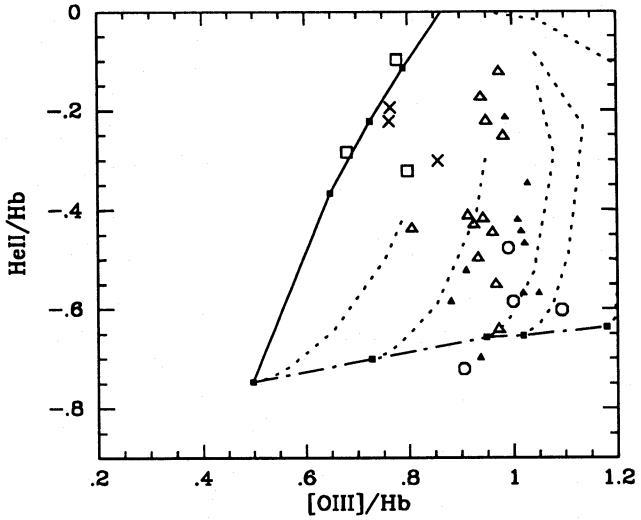

Figure 2. The He II λ4686/Hβ versus [O III] λ5007/Hβ line ratios. The notation is the same as in Fig. 1.

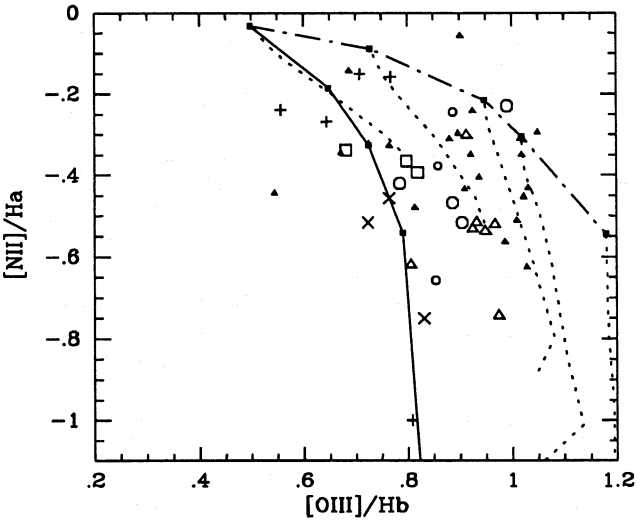

Figure 3. The [N II] λ6584/Hα versus [O III] λ5007/Hβ line ratios. The notation is the same as in Fig. 1.

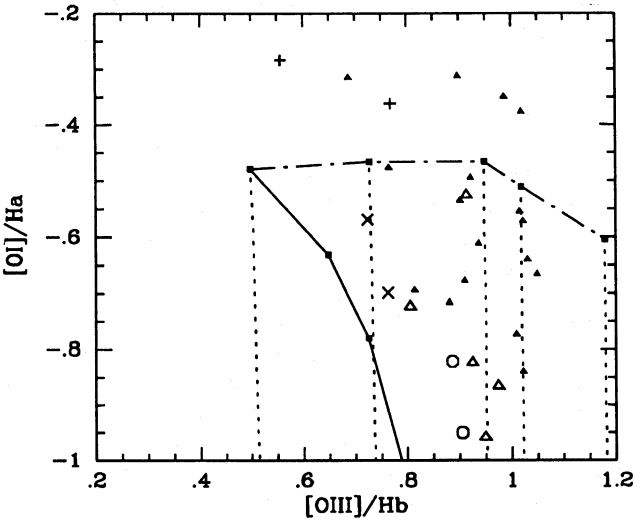

Figure 4. The [O I] λ6300/Hα versus [O III] λ5007/Hβ line ratios. The notation is the same as in Fig. 1.

As we see from the figures, most of the observational data are reproduced by photoionization models with variable τ_0. In fact, the optical depth effect mimics a variation of U when considering only optically thick models. In Fig. 1, we plot the two indicators of the gas excitation. Notice that several subregions of Cen A are not in the zone delimited by the models. This could be due to the reddening correction which tends to increase the [O II]/[O III] line ratios. If no reddening correction is made, the data are closer to the optically thick curve (see Morganti *et al.* 1991).

For a very low ionization parameter ($U=10^{-3.2}$) the behaviour of the two plotted line ratios with respect to the optical depth is similar, and leads to a variation of a factor of 2 between the optically thin and the optically thick cases. As U increases, the dependence of [O III]/Hβ on τ_0 is smaller, and the variation of the line ratio is only about 20 per cent for $U=10^{-2}$. However, the variation with τ_0 is more drastic for [O II]/[O III], leading to a change of a factor of 15 for $U=10^{-2}$. This is mainly due to the variation of the O^+ emitting volume with τ_0. Thus our first conclusion is that [O III]/Hβ is a better indicator of the excitation of the gas, and of the value of U, in AGN and EELR.

The He II λ4686 emission line is characteristic of a high-ionization zone, and we plot He II/Hβ versus [O III]/Hβ in Fig. 2. As discussed before, radiation-bounded models provide an He II/Hβ line ratio which is too low ($\simeq 0.2$) compared to the observations. On the other hand, depending on τ_0, matter-bounded models give a good fit to most of the subregion results. The smaller is τ_0, the higher is He II/Hβ.

The [O III]/Hβ ratio has a different behaviour. For $U<10^{-2.7}$, since the gas is not very ionized, O^{++} is the more abundant ion in the zone close to the illuminated edge of the emitting gas, and matter-bounded models do not affect its emitting volume, even for very low values of τ_0. For higher ionization parameters, O is more ionized and higher ions dominate the zone close to the inner edge. With decreasing τ_0 initially only the H^+-emitting volume is affected and [O III]/Hβ increases. Such an increase continues until the O^{++}-emitting volume starts to be affected, leading then to a decrease of the line ratio. The higher the value of U, the stronger the effect on [O III]/Hβ (see Fig. 2). For $U>10^{-2.5}$, [O III]/Hβ corresponding to an optically thin case is smaller than the value obtained with an optically thick model.

The low-ionization line, [N II], is shown in Fig. 3. The optically thick results for [N II]/Hα are above the observational data.

Radiation-bounded models with $10^{-3.2}\leq U\leq 10^{-2.5}$ provide a good fit to the observed line ratios. Several subregions, however, show [N II]/Hα to be still lower than the optically thin results. This point is addressed in Section 4.

The behaviour of another low-ionization line is shown in Fig. 4, where we plot [O I]/Hα versus [O III]/Hβ. As expected, the [O I] emission line is strongly affected by a reduction of the cloud's geometrical size (i.e. smaller τ_0), the [O I]/Hα line ratio increasing with τ_0. The observations give [O I]/H$\alpha>0.10$, which can be reproduced by models with $\tau_0>20$. This lower limit on τ_0 depends on U, being higher for higher U (Table 1). For this range of τ_0 values, the theoretical [O III]/Hβ ratio is already close to the optically thick results, explaining the vertical dotted curves in Fig. 4. The models with variable τ_0 fit most of the observations.

Notice that the [O I] line intensity is also dependent on the value of (H^+/H) where the model integration stops. In our case, this final value has been chosen to be 1 per cent (Binette 1985). Because a power-law ionizing spectrum produces a wide semi-ionized zone, the lower the (H^+/H) limit, the higher the [O I] emission-line intensity, even for models with τ_0 higher than 10^3, for which most of the other emission lines have already reached the optically thick value. The effect is even more important at higher U. Thus, if we were to stop the calculations when the fraction of ionized hydrogen reached only 0.1 per cent, the optically thick curve (dot–dashed line) in Fig. 4 would move upward for $U>10^{-3}$, improving the fit to the observational data.

It is well known that photoionization models fail to explain the [O III] λ4363/λ5007 line ratios observed in the EELR (Tadhunter, Robinson & Morganti 1989; Morganti *et al.* 1991). This is illustrated in Fig. 5, where we plot characteristic line ratios of the high-ionization zone of the emitting

Table 1. Theoretical line ratios.

log U	-3.2		-3.0		-2.5		-2.0	
τ_0	$\frac{HeII}{H\beta}$	$\frac{[OI]}{H\beta}$	$\frac{HeII}{H\beta}$	$\frac{[OI]}{H\beta}$	$\frac{HeII}{H\beta}$	$\frac{[OI]}{H\beta}$	$\frac{HeII}{H\beta}$	$\frac{[OI]}{H\beta}$
thin	0.38	.012	0.50	.004	0.83	–	1.03	–
1.00	0.32	.020	0.39	.008	0.60	–	0.75	–
10.0	0.20	.090	0.21	.051	0.27	.010	0.30	–
20.0	0.18	0.18	0.20	0.12	0.24	.026	0.26	.006
50.0	0.18	0.33	0.20	0.24	0.23	.065	0.24	.027
100.	0.18	0.45	0.20	0.35	0.22	0.15	.023	.051
thick	0.18	1.28	0.20	1.32	0.22	1.20	0.23	0.96

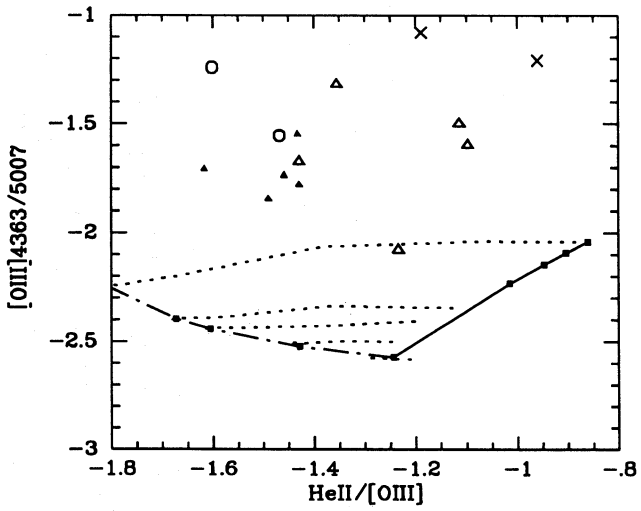

Figure 5. The [O III] λ4363/λ5007 versus He II λ4686/[O III] λ5007 line ratios. The notation is the same as in Fig. 1.

gas: [O III] λ4363/λ5007 and He II λ4686/[O III] λ5007. For optically thick models, notice that He II/[O III] line ratios increase with decreasing U. In addition, at a given value of U, the smaller the value of τ_0, the higher the He II/[O III] line ratio. On the other hand, the [O III] line ratio depends only on the value of U, and for $U \leq 10^{-2}$, which is characteristic of EELRs, the theoretical values are too low.

It turns out that photoionization by itself is insufficient to explain the strength of the observed temperature-sensitive [O III] λ4363/λ5007 ratio and, therefore, additional heating mechanisms have to be invoked. Viegas & de Gouveia Dal Pino (1992) show that the presence of shocks in the EELR can definitely improve the theoretical results, providing a better fit to the observations.

3.3 Mixing models

Matter-bounded models seem to explain the observations quite well (Figs 1 to 4). We expect, therefore, that a subregion showing high He II line intensity should have low [O I] intensity. However, this tendency is not seen in the plot of the observed [O I]/Hβ versus He II/Hβ line ratios (Fig. 6). In fact, there are several subregions of the EELRs of Cen A and 3C 227 with high He II/Hβ ratios (characteristic of optically thin regions) and high [O I]/Hβ ratios (characteristic of optically thick results). Notice that matter-bounded models give He II/Hβ > 0.25 only if $\tau_0 < 20$, but, in this case, [O I]/Hβ is lower than 0.30 (Table 1). Thus the observed values can only be matched if for each observed subregion there is a mixing between optically thick and optically thin gas. In the following, we show that a complete range of densities (from 10 to 1000 cm^{-3}) is not needed, but just two zones with a density contrast of at most 16.

Since [O I]/Hβ is higher for radiation-bounded models with lower U, and He II/Hβ is higher for matter-bounded models with higher U, we plot in all the figures the results obtained from combining two extreme cases: (i) $\tau_0 \simeq 10^4$, $U = 10^{-3.2}$, and (ii) $\tau_0 < 1$, $U = 10^{-2}$. The mixing model is represented by a solid line obtained by varying the contribution of each case to the emission-line spectrum. This solid line corresponds to a kind of limiting model. Any other combination of optically thick (low U) and optically thin (high U) would appear in the diagrams between the lines representing the mixing model (solid line) described above and the optically thick models (dot–dashed line).

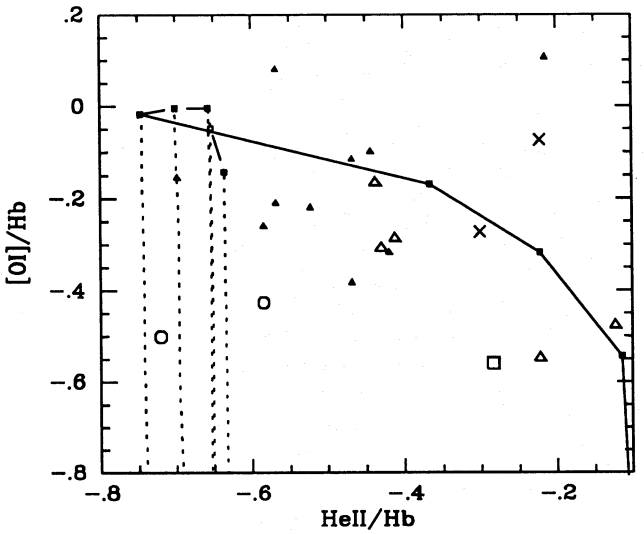

Figure 6. The [O I] λ6300/Hβ versus He II λ4686/Hβ line ratios. The notation is the same as in Fig. 1.

We see from the figures that the extreme mixing model plotted defines a sort of limit enclosing the bulk of observed values in the diagnostic diagrams. In particular, from the [O I]/Hβ versus He II/Hβ diagram (Fig. 6), a contribution of optically thick structure of at least 30 per cent to the subregion line spectrum is deduced.

Notice that the [S II] λλ6717 + 6731 emission lines have a behaviour similar to the [O I] line, since they are also produced in the transition zone. They have been observed in several subregions of Cen A, where the He II emission line is intense. However, the theoretical results for [S II] lines are not as accurate as for the other lines discussed here, especially because for the S ions the dielectronic recombination coefficients at low temperature are not available. If this mechanism is as important to the ionization equilibrium as it is for ions of the other elements, the theoretical [S II] line intensity should be higher than predicted. Thus no attempt to fit the [S II] line has been made.

An interesting point is how to interpret the mixing models with respect to the structure of the subregions. It seems clear from our results that there is obviously no necessity to have a continuous distribution of densities, as proposed by Morganti *et al.* In fact, given the density range observed in the EELR (a few $\times 10^2$ cm^{-3} or less), density variations (within this low-density range) at constant ionization parameter have no influence on the line intensities relative to Hβ. However, variations in the optical depth certainly do, as shown here.

As we see in the figures, we must combine the spectra produced by an optically thick filament and by an optically thin one, with different ionization parameters. For the limiting model plotted in the figures, the ionization parameter ratio is 16. Since U is proportional to $(nR^2)^{-1}$, the variation of U should correspond to different densities if the two zones are at the same distance from the nucleus or, if both zones have the same density, the optically thicker one should be further away from the nucleus. This latter solution would imply that some clouds are lying closer to the galactic centre, and the combined spectrum would appear only for special geometry. On the other hand, the case of both clouds at the same distance is more likely to occur in the EELR, corresponding to a situation in which the denser clouds are bathed in a more diluted gas. The spectrograph slit would then include both zones, tending to cut out a larger portion of the diluted gas. In this case, considering that the ratio between the Hβ emissivity of the optically thin to the optically thick component is about 1/170, in order to produce the same Hβ luminosity the area of the diluted gas facing the nucleus must be a factor of 170 larger than that of the dense cloud.

3.4 Interstellar dust

The He II/Hβ line ratio could also be increased by the effect of dust. Dust is probably present in the interstellar media of the host galaxies. The dust lane in Cen A is known. The nuclear radiation could be partially absorbed by dust before

reaching the EELR. Assuming that the properties of the interstellar dust in Cen A and 3C 227 are similar to those in our Galaxy, the extinction curve has a maximum at about 17 eV (Aannestad 1989), leading to a deficit of low-energy ionizing photons (i.e., photons with $E < 40$ eV). Thus, due to a lack of these photons, the Hβ line intensity in the EELR would be smaller while He II line intensity, which depends on the number of photons with $E \geq 54.4$ eV, would not change. The net effect would be an increase of the He II/Hβ ratio.

In order to mimic such a dust effect on the ionizing radiation, models considering a power-law spectrum with a low-energy cut-off have been explored, with E_c in the range 16 to 35 eV. Since in these models hydrogen is less ionized, the [O I]/Hβ line ratio can reach values much higher than observed. Thus the models stopped when [O I]/Hβ was higher than 2.

The higher E_c, the higher the He II/Hβ ratio. In particular, for $E_c = 35$ eV, He II/Hβ reaches 0.6. Actually, all the line intensities relative to Hβ are higher than in the models with no low-energy cut-off. Although the theoretical He II/Hβ line ratios seem promising, the other observed line ratios could not be reproduced by these models, and therefore should be dismissed.

4 ABUNDANCES

The chemical abundances in the EELRs could provide a clue for their origin. One would expect abundances close to solar if the gas originates in the galactic nucleus, and below-solar composition if metal-poor gas is accreted by the galaxy. Abundance determination depends on the physical processes occurring in the emitting gas, determining its physical conditions. On the other hand, the chemical composition adopted in the models directly influences the emission-line intensities, which are supposed to fit the observations. It seems therefore very important to discuss this issue here and try to disentangle the different mechanisms determining the line intensities.

The choice of the chemical composition as an input parameter in the models reflects on the temperature of the gas, then on the line intensities, but the effect is different from one emission line to another. Emission lines corresponding to chemical elements which are important gas coolants (O and C) tend to be more intense when the elemental abundance decreases due to a higher temperature of the emitting gas. On the other hand, if the element is not important for the gas cooling, its emission-line intensities tend to vary according to the elemental abundance.

In addition, blue lines are very sensitive to temperature changes. It is well known that the [O III] $\lambda 4363/\lambda 5007$ line ratio reflects the gas temperature. The higher values of the [O III] line ratio observed in the EELR indicate a high temperature of the emitting gas, and below-solar abundances have been invoked to explain these observations (Tadhunter *et al.* 1989). However, such a solution does not provide a good fit to the other observed line ratios, since all the line intensities change. In particular, models considering below-solar abundances severely affect the fitting to [O II]/[O III] (Fig. 1) and any line ratio involving the [N II] line.

In order to evaluate the effects and have a better insight on the abundances of the EELR, we have built up another two grids of photoionization models, with variable τ_0, considering both cosmic abundances (Allen 1973) and an average H II region composition (Shaver *et al.* 1983). Let us point out that $[O/H]_\odot \simeq 1.2[O/H]_C \simeq 1.6[O/H]_{H\,II}$; and $[N/O]_\odot \simeq [N/O]_C \simeq 1/7$, whereas $[N/O]_{H_{II}} \simeq 1/13$. For sake of clarity, in the following we will constrain our discussion to the optically thick models' behaviours, bearing in mind that any conclusion on the optical depth effect can be directly extrapolated from the models with solar composition and applies as well to the compositions now under discussion.

As expected, the oxygen line intensites, relative to Hβ, increase when the chemical composition changes from solar to cosmic or H II region abundances with the [O II] line intensity varying by a bigger factor than the [O I] and [O III] lines. For all the O lines, the effect is more important at low U. In Fig. 1, the curve corresponding to the optically thick models moves towards the upper right corner. It also turns out that results with H II region composition match the Cen A data.

On the other hand, the increase of the temperature in the transition zone produced by the below-solar abundance models enhances the [O I] line, and the theoretical results can lead to larger [O I]/Hα, of the order of 0.4, improving the fitting in Fig. 4.

The He II/Hβ line ratio (Fig. 2) is not very sensitive to the gas temperature and below-solar abundance models correspond to a shift of the optically thick results to the right. In this case, in order to fit the observed line ratios, we should therefore consider mixing models where the optically thick clouds have $U < 10^{-3.2}$ to compensate for the increase of the [O III] line intensity with the temperature.

Although the gas temperature is higher for the models with below-solar abundances, the variation of the [O III] $\lambda 4363/\lambda 5007$ line ratio (Fig. 5) is not enough to explain the observations. We remark that models with H II region chemical composition lead to an [O III] line ratio of about 10^{-2}, which corresponds to a lower limit of the observed values.

Finally, the behaviour of the [N II] emission line deserves further discussion. First, models adopting cosmic abundances lead to higher [N II] line intensities, because the decrease of [N/H] is compensated by a higher temperature. Thus, in Fig. 3, the curve corresponding to the optically thick models moves toward the upper right corner, and a fitting of the data would also require optically thick clouds with $U < 10^{-3.2}$. On the other hand, for models with H II region abundances, the curve corresponding to the optically thick models moves down to lower [N II]/Hα values, because the effect of decreasing [N/H] prevails. In this case, the theoretical results are lower than the observed ones for several subregions.

The effect of changing abundances is more clearly seen in the plot of [N II]/[O II] versus [O II]/[O III] (Fig. 7). The [N II]/[O II] line ratio is more sensitive to the [N/O] abundance ratio than to τ_0 effects, and the theoretical results are represented by nearly horizontal curves in Fig. 7. Models with solar and cosmic abundances give similar [N II]/[O II] line ratios ($\simeq 0.4$), and this value is higher than most of the observed values. On the other hand, for models with H II region abundances the theoretical line ratio is much smaller ($\simeq 0.16$) than most of the data.

In brief, when accounting for optical depth effects, solar or cosmic abundance models provide a better fit to the

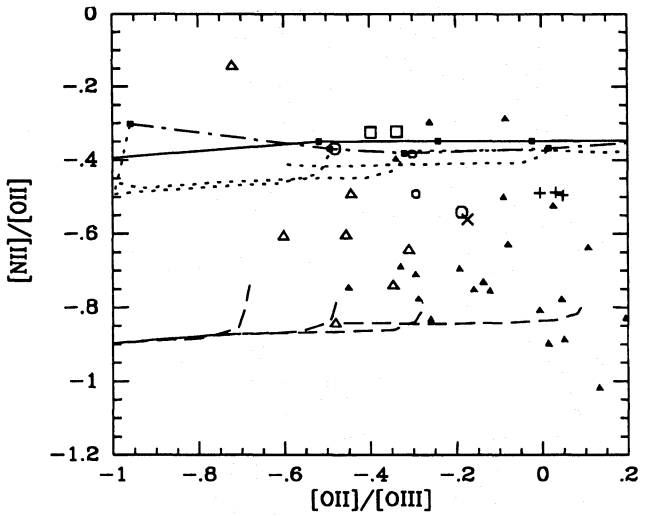

Figure 7. The [N II] λ6584/[O II] λ3727 versus [O II] λ3727/[O III] λ5007 line ratios. The notation is the same as in Fig. 1. The dashed lines correspond to optically thick models with H II region abundances.

observed line ratios. However, the scatter of the [N II]/[O II] data cannot be explained by optical depth effects and seems to indicate that the [N/O] abundance ratio must vary from solar values to 0.5 solar. Similar conclusions are reached using composite models, which account for the coupled effect of photoionization and shocks, to analyse the EELR emission-line spectra (Viegas & de Gouveia Dal Pino 1992).

5 FINAL REMARKS

From the analysis of the emission-line spectra of the EELRs of Cen A and 3C 227, we show that photoionization models, assuming a power-law spectrum for the nuclear ionizing radiation, can account for most of the line ratios only if the observed subregions are not always radiation-bounded and near-solar abundances are assumed. Two extra considerations are indeed required, first, the need for an additional heating mechanism coupled with photoionization, and secondly, below-solar nitrogen abundances. Models including the effect of dust could definitely increase both the He II/Hβ and the [O I]/Hβ line ratios, favouring the fit to the observations. Unfortunately, for the remaining line ratios the agreement with theoretical and observational data becomes worse. In the following, we comment on the main results.

Due to the optical depth effect present in most of the subregions analysed in this paper, to metallicity effects and to reddening corrections, the [O III]/Hβ line ratio is a better indicator of the excitation state of the emitting gas than the [O II]/[O III] ratio. The observed [O III]/Hβ line ratios indicate that the ionization parameter characteristic of the EELR ranges from $10^{-3.2}$ to $10^{-2.5}$. Since most of the subregions are matter-bounded, the U values give a lower limit to the number of ionizing photons produced by the nucleus. This fact enhances the well-known problem of the deficit of ionizing photons, very common in extended emission-line regions.

From the grid of models computed, we have seen that variations in the optical depth of the gas can be interpreted as variations in U in an optically thick model. Therefore the analysis of particular emission lines such as [O I] or He II is essential in order to disentangle both possibilities.

The detection of low- and high-ionization lines from the same subregion, in particular [O I] and He II emission lines, indicates that optically thick clouds are immersed in an optically thin diluted gas. The extreme case would require a density contrast of about 15 in order to explain the line ratios. Since [S II] emission lines are also produced in optically thick clouds for the subregions where their intensity ratio is available, we can have a determination of the gas density, obtaining a limit on the density of the diluted gas. Thus it emerges that the uncertainty on the number of ionizing photons required for each subregion is mainly due to the respective optical depths of the two components.

Strong support for this mixing hypothesis comes from the observed He II/Hβ trend (Fig. 2) followed by Cen A and 3C 227 subregions. Neither pure optically thick photoionization models nor photoionization coupled with shocks can reproduce it. However, optical depth variations can account for it.

Photoionization models fail to explain the high [O III] λ4363/λ5007 line ratio found in the EELR, since a large underabundance, which would increase the gas temperature, is excluded by the analysis of the other observed line ratios. This implies that an additional heating mechanism is required. The effect of shocks coupled to photoionization has been discussed elsewhere (Viegas & de Gouveia Dal Pino 1992).

The oxygen abundance is the main factor determining the temperature of the emitting gas, followed by the carbon abundance. We show that models with solar or cosmic abundances provide a better fit to the observations than those considering average H II region abundances. This means that [O/H] is about $(8\text{–}6)\times10^{-4}$, and [C/O] $\simeq$ 1/2.5. For most subregions, however, the [N/O] is between solar and half solar.

Cen A subregions require an additional remark. It seems that their reddening-corrected line ratios are better reproduced when H II region abundances are assumed. If no reddening is applied, all the data as a whole shift to the 3C 227 locus. This has important implications concerning the origin of these two EELRs, supporting, in the case of the Cen A filaments, an extranuclear origin.

Ultraviolet observations of carbon lines, which are sensitive to the gas temperature, could also provide a test of the abundances. The theoretical C III] λ1909 and C II] λ2326 line intensities, relative to Hβ, increase respectively by factors of about 4 and 2 when the chemical abundances change from solar to H II region values. On the other hand, the [N/O] abundance ratio can also be obtained from infrared observations of [N III] 57.3 μm and [O III] 51.7 μm. Photoionization models with solar or cosmic abundances lead to a [N III]/[O III] line ratio of about 0.30, whereas the ratio is 0.20 if H II region abundances are assumed. When these observations become available, they will provide a better insight into the chemical abundances in the EELR.

ACKNOWLEDGMENT

We are thankful to an anonymous referee whose helpful suggestions have contributed to improvements of this paper.

REFERENCES

Aannestad, P. A., 1989. *Astrophys. J.,* **338,** 162.

Allen, C. W., 1973. *Astrophysical Quantities,* Athlone Press, London.

Baum, C. W. & Heckman, T., 1989. *Astrophys. J.,* **336,** 702.

Binette, L., 1985. *Astr. Astrophys.,* **143,** 334.

Burns, J. O., Owen, F. N. & Rudnick, L., 1979. *Astrophys. J.,* **84,** 1683.

Burns, J. O., Feigelson, E. B. & Schreier, E. J., 1983. *Astrophys. J.,* **273,** 128.

Feigelson, E. D., Schreier, E. J., Delvaille, J. P., Giacconi, R., Grindlay, J. E. & Lightman, A. P., 1981. *Astrophys. J.,* **251,** 31.

Fosbury, R. A. E., 1989. In: *ESO Workshop on Extranuclear Activity in Galaxies,* p. 169, eds Meurs, E. J. A. & Fosbury, R. A. E., ESO Conf. and Workshop Proc. No. 32, Garching.

Grevesse, N. & Anders, E., 1989. *AIP Conf. Proc. 183 on Cosmic Abundances of Matter,* p. 1, ed. Waddington, C. J., AIP, New York.

Gruenwald, R. B. & Viegas-Aldrovandi, S. M., 1987. *Astr. Astrophys. Suppl.,* **70,** 143.

Gruenwald, R. B. & Viegas, S. M., 1992. *Astrophys. J. Suppl.,* **78,** 153.

Morganti, R., Robinson, A., Fosbury, R. A. E., di Serego Alighieri, S., Tadhunter, C. N. & Malin, D. F., 1991. *Mon. Not. R. astr. Soc.,* **249,** 91.

Pogge, R. W., 1989. In: *ESO Workshop on Extranuclear Activity in Galaxies,* p. 411, eds Meurs, E. J. A. & Fosbury, R. A. E., ESO Conf. and Workshop Proc. No. 32, Garching.

Prieto, A., di Seregho Alighieri, S. & Fosbury, R. A., 1989. In: *ESO Workshop on Extranuclear Activity in Galaxies,* p. 31, eds Meurs, E. J. A. & Fosbury, R. A. E., ESO Conf. and Workshop Proc. No. 32, Garching.

Robinson, A., Binette, L., Fosbury, R. A. E. & Tadhunter, C. N., 1987. *Mon. Not. R. astr. Soc.,* **227,** 97.

Shaver, P. A., McGee, R. X., Newton, L. M., Danks, A. C. & Pottasch, S. R., 1983. *Mon. Not. R. astr. Soc.,* **204,** 53.

Tadhunter, C. N., Robinson, A. & Morganti, R., 1989. In: *ESO Workshop on Extranuclear Activity in Galaxies,* p. 293, eds Meurs, E. J. A. & Fosbury, R. A. E., ESO Conf. and Workshop Proc. No. 32, Garching.

Viegas-Aldrovandi, S. M., 1988. *Astrophys. J. Lett.,* **330,** L9.

Viegas, S. M. & de Gouveia Dal Pino, E. M., 1992. *Astrophys. J.,* **384,** 467.

Whittle, M., 1989. In: *ESO Workshop on Extranuclear Activity in Galaxies,* p. 199, eds Meurs, E. J. A. & Fosbury, R. A. E., ESO Conf. and Workshop Proc. No. 32, Garching.